Nucleic Acids Research, 1997, Vol. 25, No. 23 **4715–4722**

A spermidine-induced conformational change of long-armed hammerhead ribozymes: ionic requirements for fast cleavage kinetics

Christian Hammann, Robert Hormes[1], Georg Sczakiel[1] and Martin Tabler*

Institute of Molecular Biology and Biotechnology, Foundation for Research and Technology Hellas, PO Box 1527, GR-71110 Heraklion, Crete, Greece and [1]Forschungsschwerpunkt Angewandte Tumorvirologie, Deutsches Krebsforschungszentrum, Im Neuenheimer Feld 242, D-69120 Heidelberg, Germany

Received August 29, 1997; Revised and Accepted October 7, 1997

ABSTRACT

The catalytic activity of the *trans* cleaving hammerhead ribozyme 2as-Rz12, with long antisense flanks of 128 and 278 nt, was tested under a wide range of different reaction conditions for *in vitro* cleavage of a 422 nt RNA transcript derived from human immunodeficiency virus type 1 (HIV-1). Depending on the reaction conditions, *in vitro* cleavage rates varied by a factor of ~100. Increasing concentrations of magnesium up to 1 M were found to enhance the reaction. Sodium when added simultaneously with magnesium showed an inhibitory effect on the cleavage reaction. Addition of sodium during pre-annealing, however, produced a stimulating effect. It was found that the additional inclusion of spermidine during pre-annealing further increased the reaction rate markedly. In accordance with accelerated cleavage, it was possible to identify a distinct, spermidine-induced conformer of the ribozyme–substrate complex. Under the most favourable conditions cleavage rates of 1/min were obtained, which are in the range of rates obtained for conventional hammerhead ribozymes with short antisense flanks. A comparison of thermodynamic data for short- and long-armed hammerhead ribozymes suggested that the activation entropy became unfavourable when helices I and III formed a long chain ribozyme–substrate complex. We conclude that in the absence of spermidine folding into the active conformation is impaired by increased friction of long helices, resulting in relatively low cleavage rates *in vitro*.

INTRODUCTION

Most hammerhead ribozymes described to date contain a catalytic core consisting of four short conserved sequence elements identical to those naturally found in some subviral pathogenic RNAs of higher plants (for reviews see 1,2). In engineered hammerhead ribozymes there is variation of the non-conserved nucleotides, especially the length of the flanking sequences, which compose the antisense part of the catalytic RNA. Hammerhead ribozymes are usually designed for multiple turnover, i.e. one ribozyme molecule cleaves several substrate RNAs in a catalytic cycle consisting of substrate association, chemical cleavage and product dissociation. In order to ensure reasonably fast dissociation, the length of the antisense arms of the hammerhead ribozyme (helix I and III) must not exceed ~10 complementary bases (3).

In our own work we have used hammerhead ribozymes with much longer antisense sequences (>100 nt) flanking the catalytic domain. Due to their resemblance to ordinary antisense RNA, we called such ribozymes ‘catalytic antisense RNA’ (4). Their association with the substrate RNA proceeds in a way similar to conventional antisense RNA. A minimal kinetic reaction scheme for catalytic antisense RNAs is given in Figure 1. Unlike conventional hammerhead ribozymes, catalytic antisense RNAs are thought to cleave their substrate RNA in a stoichiometric manner, since product dissociation cannot be expected. However, catalytic antisense RNA was more effective than non-catalytic antisense control RNA in inhibiting replication of human immunodeficiency virus type 1 in living cells (6,7). An ensuing study has shown that asymmetric hammerhead ribozymes with a long helix III in combination with a helix I of as little as 3 nt can be equally efficient *in vitro* as well as in living cells (8). Recently catalytic antisense RNA was compared with conventional short hammerhead ribozymes for its inhibitory effect on HIV-1 replication. It was found that long-armed hammerhead ribozymes were highly efficient in inhibiting HIV-1 replication when micro-injected into the nucleus of human cells, whereas ribozymes with short antisense arms were almost ineffective. Conversely, short chain ribozymes were superior to long-armed when micro-injected into the cytoplasm (9).

The *in vitro* cleavage reaction of short-armed hammerhead ribozymes (Fig. 1) has been studied in great detail (10,11). For those ribozymes that follow Michaelis–Menten kinetics the overall efficiency is most commonly characterized by the ratio of the catalytic constant k_{cat} to the Michaelis constant K_m, which approximates the dissociation constant of the double-stranded complex formed between ribozyme and substrate RNA. The value of k_{cat}/K_m combines binding and cleavage properties and allows a comparison of the efficiency of different ribozyme–substrate pairs. However, the use of Michaelis–Menten kinetics requires that the concentration of the ribozyme–substrate complex is constant and that product dissociation is not rate limiting.

*To whom correspondence should be addressed. Tel: +30 81 394365; Fax: +30 81 394408; Email: tabler@nefeli.imbb.forth.gr

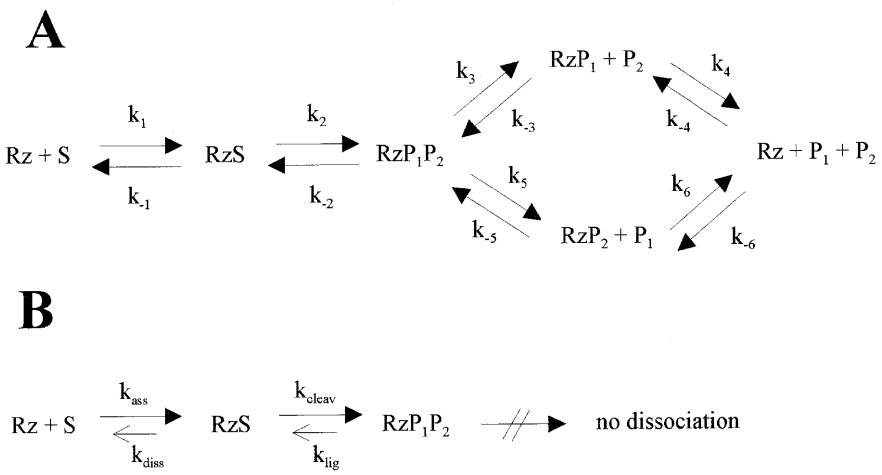

Figure 1. Minimal kinetic reaction schemes for differently designed hammerhead ribozymes. Rz denotes the ribozyme, S the substrate and P_1 and P_2 the products of the cleavage reaction. (**A**) Conventional, short-armed hammerhead ribozymes according to Baidya and Uhlenbeck (5). (**B**) Catalytic antisense RNAs. Due to the long antisense flanks, the dissociation constant k_{diss} is close to zero. We do not have any indication that a ligation step occurs in the case of catalytic antisense RNAs (Hammann and Tabler, unpublished results) and cleavage is found to be quantitative.

Thus it is not possible to apply the Michaelis–Menten reaction scheme to catalytic antisense RNA, since the double-stranded complex will not dissociate (the dissociation constant k_{diss} is close to zero). Instead, the performance of catalytic antisense RNA is described by the rate of association with the substrate RNA and by the cleavage rate. Cleavage rates (k_{cleav}) are determined under single turnover conditions, using a preformed complex between catalytic antisense RNA and its substrate. The cleavage rates observed in previous studies were of the order of 0.01/min (6,12,13), which was ~100 times slower than the k_{cat} values typically observed for conventional hammerhead ribozymes (2). It has been previously discussed (12) that these substantial differences could be due to a conformational change preceding the actual chemical cleavage step. The objective of the current study was to find out whether there are experimental conditions which would accelerate such a presumed conformational change, so that hammerhead ribozymes with long antisense flanks would be able to cleave their substrate RNA at rates comparable with conventional hammerhead ribozymes.

MATERIALS AND METHODS

Unless stated otherwise, all molecular procedures were performed as described by Sambrook *et al.* (14).

Synthesis of substrate, antisense and ribozyme RNA

Plasmids pBS29-CX and pBS29-Rz12 have been described previously (6) and were used for *in vitro* synthesis of target RNA 2s, antisense RNA 2as and of ribozyme 2as-Rz12. *In vitro* synthesis of radioactively labelled target RNA 2s was carried out in a total volume of 20 µl containing 40 mM Tris–HCl, pH 8.0, 20 mM $MgCl_2$, 5 mM dithiothreitol, 40 U RNase inhibitor (Boehringer, Mannheim, Germany), 1 µg/ml BSA, 500 µM each ATP, CTP and GTP, 15 µM UTP, 2.5 µM [α-^{32}P]UTP (800 Ci/mmol) and 1 µg *Hin*dIII-linearized pBS29-CX. The reaction was started by addition of 40 U T7 RNA polymerase (MBR, Milwaukee, WI) and incubated for 1.5 h at 37°C. *In vitro* transcription reactions for antisense RNA 2as and for ribozyme RNA 2as-Rz12 were carried out in a total volume of 100 µl containing 40 mM Tris–HCl, pH 7.5, 6 mM $MgCl_2$, 10 mM dithiothreitol, 4 mM spermidine, 40 U RNase inhibitor, 1 µg/ml BSA, 1 mM each ATP, CTP, GTP and UTP and 5–7 µg *Sac*I-linearized pBS29-CX or *Sac*I-linearized pBS29-Rz12 respectively. The reaction was started by addition of 60 U T3 RNA polymerase (MBR) and run for 2.5 h at 37°C. Both reactions were stopped by addition of 10 U DNase I (RNase-free) (Boehringer). After a further incubation for 15 min at room temperature each mixture was subjected to a phenol extraction and purified by gel filtration on a 2 ml column containing Biogel A-50 (BioRad, Richmond) that had been equilibrated previously with TE buffer. The purity of the radiolabelled target RNA 2s was confirmed on a 5% denaturing polyacrylamide gel (15) and its concentration determined by scintillation counting. After gel filtration the transcripts 2as and 2as-Rz12 were ethanol precipitated and the pellets washed twice with 70% ethanol. The dried pellets were redissolved in 20 µl water and the purity of the transcripts was confirmed using a 5% denaturing polyacrylamide gel. Recovery ranged between 20 and 35 µg and was determined spectrophotometrically, assuming that 1 absorbance unit at 260 nm corresponds to 40 µg/ml RNA in a 1 cm path length cell.

Magnesium dependence

^{32}P-Labelled 2s (2–4 nM) and 2as-Rz12 (20–50 nM) were incubated separately in 25 mM Tris–HCl, pH 7.4, and 100 mM NaCl at 90°C for 1 min, mixed and pre-annealed overnight at room temperature. All components of the cleavage reaction were incubated for 3 min at 37°C. From 30 µl containing pre-annealed RNA a 3 µl aliquot was removed and kept as a zero value. The cleavage reaction was started by addition of 3 µl various $MgCl_2$ stock solutions to give final Mg^{2+} concentrations of 0.3, 0.6, 1, 2, 3, 6, 10, 20, 30, 60, 100 and 300 mM. For high final Mg^{2+} concentrations (600, 1000 and 1666 mM) appropriate $MgCl_2$ solutions were mixed with pre-annealed RNA at a 1:2 ratio. At appropriate time points 3.5 µl aliquots were withdrawn and added to stop buffer, the EDTA content of which was adjusted for the

appropriate magnesium concentration. The samples were subjected to ethanol precipitation and pellets redissolved in 15 µl gel loading buffer. The samples were denatured at 100°C for 5 min and subsequently cooled on ice. The reaction products were separated on 6% denaturing polyacrylamide gels. The dried gels were scanned and quantified using a PhosphorImager (Molecular Dynamics) and the program ImageQuant. For each time point the percentage of cleavage was determined. Cleavage rates constants k_{cleav} were determined for the first rate of the biphasic reaction according to pseudo-first order kinetics using Microcal Origin. Each experimental set-up was repeated at least once and errors in measurement were <20%. These procedures were also applied in all other kinetic experiments unless stated otherwise.

Temperature dependence

The pH of the Tris buffer was adjusted for each temperature. Reaction mixtures and $MgCl_2$ solutions were pre-incubated for 5 min at the indicated temperatures (4, 20, 25, 30, 37, 40, 45, 50, 55, 60, 65 and 70°C). After removal of a 3 µl aliquot as a zero value the reaction was started by addition of $MgCl_2$ to the RNA mixtures, giving a final concentration of either 10 mM or 1 M. Aliquots of 3 µl were withdrawn at appropriate time points and mixed with 30 µl stop solution (50 mM Tris–HCl, pH 8.0, and 50 mM EDTA or 250 mM EDTA for experiments containing 10 mM or 1 M $MgCl_2$ respectively).

Determination of thermodynamic parameters

The Arrhenius activation energy (E_a) was calculated from an Arrhenius plot (ln k_{cleav} versus $1/T$) derived from the temperature dependence of the cleavage reaction, which was found to be linear between 4 and 45°C for 10 mM Mg^{2+} and between 4 and 50°C for 1 M Mg^{2+} (data not shown). The Gibbs's free activation enthalpy ($\Delta G^{\ddagger}$) was calculated from the relationship $\Delta G^{\ddagger} = -RT\ln(kh/k_BT)$ where R is the gas constant, k is the rate constant at the given temperature T, h is Planck's constant and k_B is Boltzmann's constant. The activation enthalpy ($\Delta H^{\ddagger}$) is given by $\Delta H^{\ddagger} = E_a - RT$ and the activation entropy ($\Delta S^{\ddagger}$) was calculated from the relationship $\Delta G^{\ddagger} = \Delta H^{\ddagger} - T\Delta S$. Entropy values are given in eu (cal/mol K); one eu is equivalent to 4.184×10^{-3} kJ/mol K.

Sodium dependence

Two different procedures were applied. In the first series of simultaneous experiments RNA duplex was preformed in the absence of ions, except those present in the pre-annealing buffer. The cleavage reaction was started by simultaneous addition of Mg^{2+} and Na^+ at various concentrations. In the second series of sequential experiments RNA duplex was pre-formed in the presence of various concentrations of Na^+ and the cleavage reaction was started by addition of Mg^{2+} alone at various concentrations. Both types of experiments were repeated in the presence of 2.5 mM spermidine. Radioactively labelled RNA 2s (0.4 nM) and at least a 100-fold excess of ribozyme RNA 2as-Rz12 (>40 nM) were mixed in a total volume of 200 µl containing 50 mM Tris–HCl, pH 8.0, and 5 mM EDTA. For the spermidine experiments 2.5 mM spermidine was added. The pH of the buffer solution (50 mM Tris–HCl, 5 mM EDTA, pH 8.0) was not significantly changed upon addition of spermidine at final concentrations <5 mM. For the series of simultaneous experiments 8 µl aliquots of the 200 µl mixture were individually subjected to a slow cooling procedure from 94 to 37°C, which lasted ~1 h. For the sequential experiments 2 µl NaCl-containing solution were added to the 8 µl aliquots before the slow cooling procedure, giving final concentrations of 0, 5, 50 and 500 mM Na^+. Complete duplex formation was monitored by 5% denaturing polyacrylamide gel electrophoresis, without boiling the samples before loading, as the duplex RNA does not melt on its own in a denaturing gel due to the long complementary flanks of catalytic antisense RNA. An aliquot of 1.5 µl was withdrawn as a zero value for each individual set-up and the reaction started by addition of various amounts of $MgCl_2$, compensating for the EDTA from the hybridization step and giving final concentrations of free Mg^{2+} of 5, 50 and 100 mM (sequential experiments), or in the simultaneous experiments by addition of NaCl/$MgCl_2$ salt mixtures, in all combinations of $[Na^+]$ = 0, 5, 50 or 500 mM and $[Mg^{2+}]$ = 5, 50 or 100 mM (final concentrations). Sequential and simultaneous experiments were also performed in the presence of 2.5 mM spermidine in the slow cooling mixture. All kinetic measurements were carried out at 37°C. At at least five appropriate time points aliquots were withdrawn from the mixture and added to 200 µl precooled stop solution (0.2 M NaOAc, pH 5.3, 4 mM EDTA, 50 µg/ml yeast carrier RNA). For separation of cleavage products 5% denaturing (8 M urea) polyacrylamide gels were used.

Detection of a spermidine-induced conformer

In a slow cooling procedure in 50 mM Tris–HCl, 5 mM EDTA, pH 8.0, an excess of ribozyme 2as-Rz12 or antisense RNA 2as over radiolabelled substrate RNA 2s was used to form double-stranded complexes. Without boiling the two duplexes were loaded on a 5% polyacrylamide gel containing 8 M urea in order to separate the duplexes from non-annealed ribozyme or antisense RNA. The duplex RNAs were excised and the purified complexes recovered by electroelution. After phenol extraction and NaOAc/EtOH precipitation the complexes were dissolved in 50 µl H_2O. Aliquots of 4 µl of the purified complexes were incubated separately for 10 min at 37°C in 50 mM Tris–HCl, 5 mM EDTA, pH 8.0, in a total volume of 10 µl. As an additional control a radiolabelled DNA marker was also incubated in this solution. The complexes and the DNA marker were also incubated in the same buffer additionally containing 2 mM spermidine. After incubation the samples were put on ice for 5 min and loaded directly on a native 3.5% polyacrylamide gel containing 0.1% Triton X-100 and 2 mM spermidine. The same concentration of spermidine was also used in the running buffer. In order to ensure fast migration into the gel matrix, loading was performed at 8 V/cm at a power of 3 W (limiting). Gels were run under these conditions for 8 h at room temperature. The same procedure was also performed on a gel system which was lacking spermidine in both the gel and the running buffer (data not shown).

RESULTS

In the current study we tested the cleavage behaviour of the catalytic antisense RNA 2as-Rz12 under different reaction conditions. This previously described ribozyme (6) contains a 5′ antisense flank (helix I) of 128 nt and a 3′ antisense flank (helix III) of 278 nt and was directed against the substrate RNA 2s, corresponding to the 5′ leader/*gag* region of HIV-1. In all experiments the substrate RNA 2s was radioactively labelled and

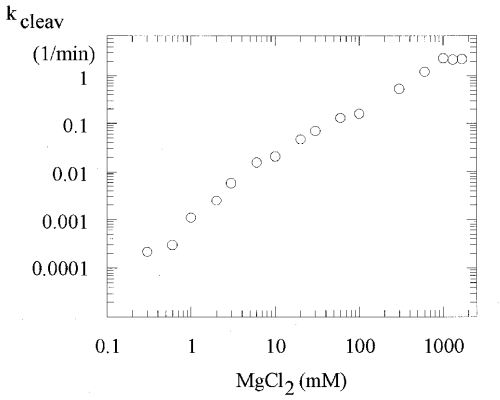

Figure 2. Cleavage rates depending on the magnesium concentration. The cleavage reactions were carried out at 37°C in 25 mM Tris–HCl, pH 7.4, 100 mM NaCl and Mg^{2+} concentrations as indicated. The values represent the average of at least two measurements.

the ribozyme RNA 2as-Rz12 was used in molar excess. These two RNAs were annealed to form the double-stranded complex, thus excluding any influence of the association step on cleavage. The cleavage reaction itself was initiated by addition of Mg^{2+}-containing start solutions. Due to the long antisense arms the two cleaved product RNAs remained hybridized with the ribozyme strand, excluding any influence of dissociation on the observed cleavage rates.

Influence of magnesium on the cleavage reaction

After preforming the 2as-Rz12/2s ribozyme–substrate complex in 25 mM Tris–HCl, pH 7.4, cleavage was carried out in the presence of Mg^{2+} concentrations ranging between 0.3 mM and 1.7 M. As shown in Figure 2, the cleavage rate was greatly increased by elevated concentrations of Mg^{2+}, with no apparent maximum up to 1 M. In this respect catalytic antisense RNAs are distinct from conventional hammerhead ribozymes, for which different magnesium dependencies have been described. However, enhanced cleavage usually approached a maximum at <100 mM Mg^{2+} (16–21).

In a second set of experiments the ribozyme–substrate complex RNA was allowed to form in the presence of various amounts of sodium and the reaction started by addition of magnesium only (sequential addition, Fig. 4). At low Mg^{2+} concentrations the inhibitory effect of Na^+ remained. However, at higher Mg^{2+} concentrations we found a stimulating effect of Na^+, opposite to what was observed for simultaneous application of magnesium and sodium.

The cleavage reaction of 2as-Rz12 is characterized by an unfavourable activation entropy

In view of the differences in cleavage behaviour between catalytic antisense RNA and conventional short-armed hammerhead ribozymes observed under standard reaction conditions we determined thermodynamic values of the cleavage reaction. Cleavage rates of 2as-Rz12/2s were measured at different temperatures, ranging from 4 to 70°C. The activation energies were determined and were compared with those published for the two short hammerhead ribozymes HH16 (11) and HHRz (22). The thermodynamic parameters for the three ribozymes are summarized in Table 1 and show that the energy barrier represented by the Gibb's free activation enthalpy ($\Delta G^{\ddagger}$) was increased for the long chain and slow cleaving ribozyme–substrate complex. The value of $\Delta G^{\ddagger}$ for 2as-Rz12/2s was not influenced by association, as an annealed complex was used. The difference in ΔG between the long-armed and the short-armed hammerhead ribozymes was of the order of ~3 kcal/mol (Table 1). Since the activation enthalpy ($\Delta H^{\ddagger}$) was actually smaller for 2as-Rz12/2s, the increase in $\Delta G^{\ddagger}$ was caused by an unfavourable activation entropy ($\Delta S^{\ddagger}$) compared with the two short-armed hammerhead ribozymes.

Influence of sodium on the cleavage reaction

In a first set of experiments we allowed formation of the ribozyme–substrate complex to occur in the absence of any added metal ions (disregarding the sodium originating from buffered EDTA). Complete double-strand formation was confirmed by gel shift analysis (data not shown). The cleavage reaction was started by addition of several combinations of Na^+ and Mg^{2+}, as shown in Figure 3 (simultaneous addition). For all three Mg^{2+} concentrations tested (5, 50 and 100 mM) we observed an inhibitory effect with increasing concentrations of Na^+. The combination of low Mg^{2+} and high Na^+ concentrations especially resulted in poor cleavage ($k_{cleav} \approx 0.01$/min).

Table 1. Comparison between the thermodynamic parameters of catalytic antisense RNA 2as-Rz12 and two published short-armed hammerhead ribozymes

Ribozyme/ substrate	Helices I/III (nt/nt)	Substrate (nt)	Temperature (K)	$[Mg^{2+}]$ (mM)	k_{cleav} (1/min)	E_a (kcal/mol)	$\Delta G^{\ddagger}$ (kcal/mol)	$\Delta H^{\ddagger}$ (kcal/mol)	$\Delta S^{\ddagger}$ (cal/mol K)
HH16/S[a]	8/8	17	298	10	1	22 ± 1	20 ± 1	21 ± 1	3 ± 0.2
HHRz/S[b]	5/5	11	308	25	1	16	19.9	15.4	–14.6
2as-Rz12/2s[c]	128/278	422	298	10	0.006 ± 0.0003	11.3	22.9	10.7	–41.0
2as-Rz12/2s[c]	128/278	422	310	10	0.02 ± 0.001	11.3	23.1	10.6	–40.1
2as-Rz12/2s[c]	128/278	422	298	1000	0.47 ± 0.05	9.9	20.3	9.4	–36.8
2as-Rz12/2s[c]	128/278	422	310	1000	1.3 ± 0.5	9.9	20.5	9.3	–36.1

[a]From Hertel and Uhlenbeck (11).
[b]From Takagi and Taira (22).
[c]This study.

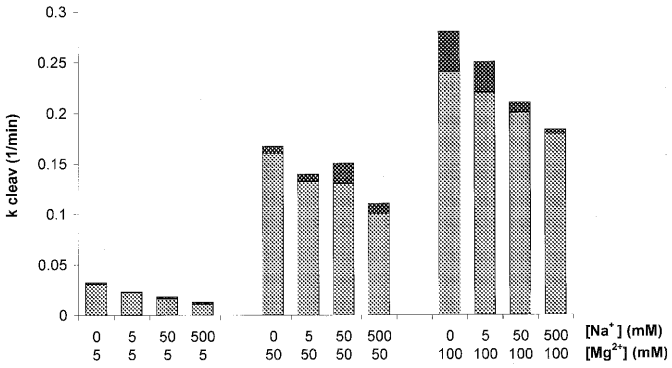

Figure 3. Cleavage rates after simultaneous addition of various concentrations of magnesium and sodium to the preformed ribozyme–substrate complex. The height of the lighter shading represents the average cleavage rate of at least two measurements; errors are indicated by dark shading. Cleavage reactions were carried out in 50 mM Tris–HCl, pH 8.0, at 37°C. As a consequence of the change in pH, the cleavage rates are higher than the equivalent ones shown in Figure 2, in agreement with the pH dependency of the hammerhead ribozyme reaction as described (18).

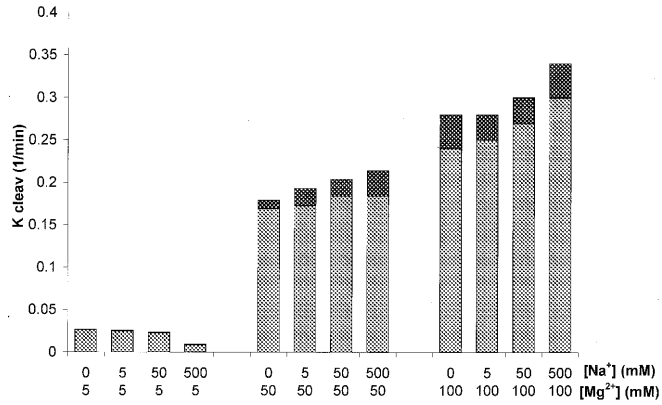

Figure 4. Cleavage rates after ribozyme–substrate duplex formation in the presence of the indicated concentrations of sodium and reaction start by addition of the indicated concentrations of magnesium (sequential addition). The height of the lighter shading represents the average cleavage rate of at least two measurements; errors are indicated by dark shading. Cleavage reactions were carried out in 50 mM Tris–HCl, pH 8.0, at 37°C.

Since simultaneous and sequential addition of metal ions resulted in the same concentrations, the observed differences in cleavage rates were not caused by variations in ionic strength. Stimulation of cleavage could indicate that sodium, if present during hybridization, is able to stabilize a more favourable complex. However, if sodium was added after complex formation, it seemed to compete with magnesium for its binding site(s). This competitive effect was always detectable after simultaneous addition, but also after sequential addition if low Mg^{2+} concentrations were applied. These data suggested that Na^+ had both a stimulating and an inhibitory effect on cleavage. Which of the two opposing effects prevailed depended on concentration of Mg^{2+} and mode of addition. Similar effects were observed for potassium (R.Hormes, unpublished results).

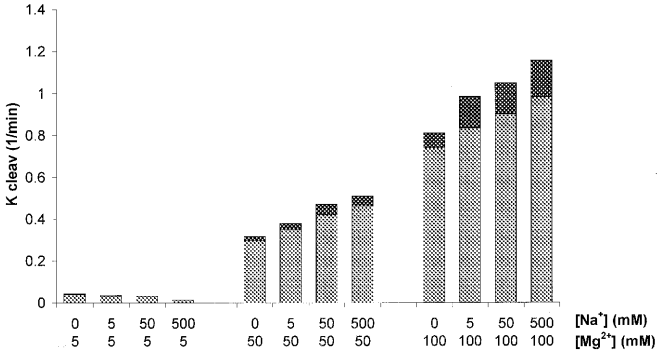

Figure 5. Cleavage rates in the presence of spermidine: 2.5 mM spermidine was included during ribozyme–substrate duplex formation and during the cleavage reaction. Both simultaneous and sequential addition of sodium and magnesium were applied (concentrations as indicated). No significant differences in cleavage rate due to mode of application (simultaneous versus sequential) were observed, so only one data set is shown. The height of the lighter shading represents the average cleavage rate of at least two measurements; errors are indicated by dark shading. Cleavage reactions were carried out in 50 mM Tris–HCl, pH 8.0, at 37°C.

Influence of spermidine on the cleavage reaction

The observed differences in cleavage rate depending on the conditions of pre-annealing prompted us to examine complex formation under the influence of the polycation spermidine, known to stabilize higher order nucleic acid structures (23). We repeated both series of experiments; simultaneous and sequential addition of sodium and magnesium in the presence of 2.5 mM spermidine in the pre-annealing buffer and during the reaction. Since Dahm and Uhlenbeck (17) showed that a related oligoamine, spermine, was able to promote cleavage in the absence of added metal ions, we tested for a spermidine-induced cleavage product, which we could not detect, even when concentrations of up to 5 mM spermidine were applied (data not shown), similar to a recent report by Kuimelis and McLaughlin (24), who found the same result for spermine.

The presence of spermidine during complex formation resulted in significantly enhanced cleavage rates, especially at high Mg^{2+} concentrations. Unlike pre-annealing in the absence of spermidine, we did not observe differences in cleavage rates between sequential or simultaneous application of sodium. Only one data set is given in Figure 5. Na^+ had a synergistic effect to spermidine and resulted in further acceleration of the reaction, but only at high Mg^{2+} concentrations. Conversely, the inhibitory effect of Na^+ still dominated at 5 mM Mg^{2+}. At the most favourable condition tested (2.5 mM spermidine, 500 mM Na^+, 100 mM Mg^{2+} or at extremely high Mg^{2+} concentration alone) we determined cleavage rates of 1/min, which is in the range of those observed for conventional hammerhead ribozymes.

Spermidine induces a conformational change in the ribozyme–substrate complex

We intended to test whether the significantly enhanced cleavage rates in the presence of spermidine were due to a conformational change and tried to trap distinct conformers. The complex between substrate RNA 2s and ribozyme 2as-Rz12 was pre-formed by a slow cooling procedure in 50 mM Tris–HCl, 5 mM EDTA, pH 8.0. As a control, a duplex RNA was formed with the comparable antisense

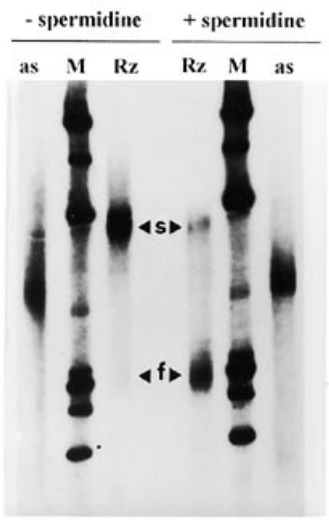

Figure 6. The ribozyme–substrate complex undergoes a conformational change in the presence of spermidine. The preformed antisense–target duplex (as) and the ribozyme–substrate duplex (Rz), as well as control marker DNA (M), were incubated for 10 min in 50 mM Tris–HCl, 5 mM EDTA, pH 8.0, at 37°C. Spermidine (2 mM) was included as indicated. Samples were directly loaded on a 3.5% polyacrylamide gel containing 0.1% Triton X-100 and 2 mM spermidine. In accordance with Gast and Hagerman (25), spermidine had little effect on the electrophoretic behavior of double-stranded RNA and the double-stranded RNA (as) and the control DNA marker are shifted only very slightly due to reduced effective charges. The ribozyme complex (Rz), however, migrated much faster in the presence of spermidine. Notably, both the slow (s) and the fast (f) migrating conformations of the ribozyme–target complex are visible in the presence and absence of spermidine, however, in inverted proportions.

RNA 2as, which differs from the ribozyme only by the absence of the catalytic domain (6). Both complexes were gel purified. The recovered complexes were incubated for 10 min in the same buffer as used for hybridization, however, in one aliquot this buffer was supplemented with 2 mM spermidine. The complexes were loaded on a native polyacrylamide gel containing 2 mM spermidine. Loading was done with applied low voltage to ensure rapid migration into the gel matrix. Under these conditions it became evident that spermidine induced a conformational change in the pre-formed ribozyme–substrate complex (Fig. 6). The complex that had not been exposed to spermidine migrated slower than the related duplex RNA, as expected. Addition of spermidine to the buffer, however, resulted in a ribozyme complex with much higher electrophoretic mobility. This complex migrated even faster than the unstructured control duplex RNA. A comparable analysis on a polyacrylamide gel without spermidine showed only the slow migrating conformation of the ribozyme complex (data not shown), indicating that the fast migrating complex depends on the presence of spermidine. We conclude that accelerated cleavage in the presence of spermidine is correlated with the conformational change in the ribozyme–substrate complex that we have described here.

DISCUSSION

In previous studies cleavage rates of catalytic antisense RNAs were ~100 times lower (12,13) than those observed for conventional hammerhead ribozymes, which have been studied in great detail (10). In view of the successful *in vivo* applications of catalytic antisense RNA, we were interested to find out whether more favourable reaction conditions for catalytic antisense RNA exist. In all our previous experiments we had included substantial amounts of NaCl (100–500 mM) to support RNA–RNA hybridization, as has been described for association studies with conventional antisense RNAs (26). In the current study we could show that Na^+ had a strong inhibitory effect on the cleavage reaction, if used in combination with a moderate Mg^{2+} concentration. We could also show that catalytic antisense RNA requires high concentrations of Mg^{2+} for maximal cleavage activity and that addition of spermidine induced a conformational change, greatly enhancing the reaction and approaching *in vitro* cleavage rates similar to those of conventional hammerhead ribozymes. In retrospect, it is evident that we had previously used unfavourable reaction conditions for determination of cleavage rates, for example for the comparative analysis of different cleavage motifs (27).

Influence of magnesium

A striking observation was that the cleavage rate obtained with catalytic antisense RNA 2as-Rz12 increased with increasing magnesium concentration, without reaching saturation up to highly unphysiological concentrations of 1 M Mg^{2+}. In contrast, it has been reported that cleavage rates of conventional all-RNA hammerhead ribozymes reached plateaux at ~20 (16,17), 100 (28,29) and exceptionally also increased up to 200 mM $MgCl_2$ (30), whereas in another study the cleavage rates did not vary between 10 and 50 mM Mg^{2+} (19).

Previous studies have shown that magnesium has multiple functions in RNA cleavage by hammerhead ribozymes (reviewed in 31). Besides its role as a catalytic cofactor, it is thought to be involved in proper folding and general electrostatic interaction to shield the phosphodiester backbone (17,32–37). Since the actual chemical cleavage step is expected to be independent of the length of the antisense arms, the increased requirement for magnesium suggests that the long arms of catalytic antisense RNA impair proper folding into the active complex.

Influence of sodium

Our data showed that sodium was unable to replace magnesium in its structural role, however, it apparently supported neutralization of the negative phosphate charges, thereby slightly increasing cleavage activity. In accordance with this, it had been shown previously for conventional hammerhead ribozymes that sodium has negligible impact on the structure (35,38,39). Neither could sodium interfere with magnesium-induced folding of the ribozyme–substrate complex (35; Fig. 7). Therefore, we interpret the inhibitory effect of sodium, particularly observed at low Mg^{2+} concentrations or with simultaneous addition, as competition for the active site. Possibly, monovalent Na^+ does not compete with Mg^{2+} but with its hydroxylated form $Mg(OH)^+$, which is generally accepted as the actual catalyst (18). This competition, however, could be overcome by increased Mg^{2+} concentrations. For conventional hammerhead ribozymes an inhibitory effect of sodium was seen in some cases (40) but not in others (16,32) and a dual effect of inhibition and stimulation has also been observed (Dr P.Hendry, personal communication, quoted in 41).

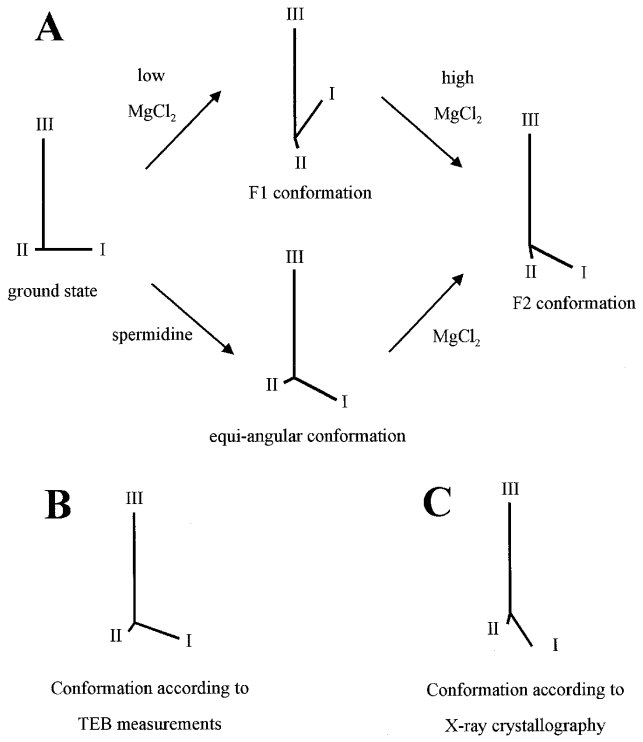

Figure 7. Highly schematic representation of the different ribozyme–target conformations applied to the RNA pair 2as-Rz12/2s, having long helices I (128 nt) and III (278 nt). (**A**) Conformations according to gel shift experiments (35,36; D.M.J.Lilley, personal communication). In the presence of spermidine alone the complex undergoes a conformational change from the ground state, seen at 2.5 mM EDTA or 50 mM NaCl, into an equiangular arrangement of the three helices, which is converted into the F2 conformation upon addition of magnesium. Notably, the ground state conformation does not change significantly upon addition of sodium (35). (**B**) The arrangement of the three helices as determined by TEB investigations (32,33). (**C**) Arrangement of the three helices as deduced from X-ray crystallography (44,46,48).

Influence of spermidine and structural implications

Biological oligoamines, such as spermine and spermidine, are able to stabilize higher order nucleic acid structures at low millimolar concentrations (23). For a conventional hammerhead ribozyme Dahm and Uhlenbeck (17) reported an ~2-fold stimulation of cleavage with 0.5 mM spermine, approaching a maximum cleavage rate at ~10 mM Mg^{2+}. We could show here that spermidine induced a conformational change in the complex formed by substrate RNA and catalytic antisense RNA. Apparently, this spermidine-induced transition resulted in a dramatic increase in cleavage activity at high Mg^{2+} concentrations compared with previous *in vitro* assay conditions (6). A similar synergistic effect of magnesium and spermidine was previously observed for catalytic M1 RNA of RNase P (42). Since most residues of the ribozyme–substrate complex are part of double-stranded helices, conformational changes are expected to originate from the unpaired nucleotides within the catalytic domain which influence the spatial array of the three helices. Two helices of the complex used in this study were long (128 and 278 bp). Since such long regions of dsRNA are relatively stiff (43; G.Steger, personal communication), structural changes influencing the angles between helices I and III can be monitored by changes in electrophoretic mobility. It was found that incubation of the pre-annealed ribozyme–substrate complex in spermidine resulted in a higher gel electrophoretic mobility and thus a compaction of form. Despite the spermidine-induced conformational change, which correlated with increased cleavability, the reaction remained dependent on the concentration of magnesium. This indicates that the spermidine-induced conformation and the active conformation were distinct, however, transition into the active conformation became easier.

Recently several independent studies have been dedicated to analysis of the structure of the hammerhead ribozyme–target complex (33,34,44–46). Using gel shift experiments Bassi *et al.* (35) showed that, induced by and depending on the concentration of magnesium, the complex folded into two different conformations with distinct angles between the three helices, as shown in Figure 7A. The structure observed in the presence of ≥2 mM Mg^{2+} remained unchanged after addition of 0.5 mM spermidine. However, in the presence of spermidine alone (besides Tris–borate buffer) an additional, distinct conformation was detectable, in which the three helices were arranged with approximately equal angles between them (D.M.J.Lilley, personal communication). This conformational change is depicted in Figure 7A. Most likely the spermidine-induced conformations observed by Lilley and in this study are closely related. It is not clear whether this ‘equiangular’ conformation is an intermediate between the inactive conformation that Bassi *et al.* (35) detected in the absence of magnesium and the fully folded (F2) structure detectable in ≥2 mM Mg^{2+}, which is consistent with the Y-like structure known from X-ray crystallography (44,46), FRET experiments (45) and TEB investigations (33,34) and which is summarized in Figure 7B and C. However, when magnesium is added to the complex incubated with spermidine, it folds into the F2 structure. Despite general agreement on the Y-like conformation of the substrate–ribozyme complex, the relative orientation of the three stems shows some discrepancies. The two studies of Amiri and Hagerman (33,34) were the first to apply unmodified all-RNA molecules for the determination of global hammerhead structure. Interestingly, they determined an angle of 116° between helices I and III (47), which is 15–27° less than the angles between helices I and III found in the crystal structure (44). As indicated in Figure 7, this conformation is closer to the ‘equiangular’ structure communicated by Lilley. On the other hand, Scott *et al.* (48) showed, for an unmodified all-RNA complex by time-resolved X-ray crystallography, that the ribozyme is able to cleave even when crystallized. It therefore seems that there are several closely related conformations that allow cleavage. The ‘ground state’, however, which strongly deviates from the active conformation(s), as depicted in Figure 7, does not allow cleavage and has to be converted into the active conformation.

It is evident that an intramolecular transition which requires changes in the angles between the three helices prior to cleavage is impaired by long helices I and III, whereas it should be less restrained in the case of short-armed hammerhead ribozymes. The interpretation of a negative influence of extended helices on the dynamic properties of the entire RNA–RNA complex is also in agreement with the observed increased difference in entropy state ($\Delta S^{\neq}$) between the uncleaved 2as-Rz12/2s complex and a high energy intermediate (Table 1). However, it is difficult to correlate the activation entropy with the structure–function relationship of the cleavage reaction. Moreover, the pH dependence of the cleavage

rate for ribozyme 2as-Rz12 was similar to that determined for conventional hammerhead ribozymes (data not shown), which is an indication that the chemical step is rate limiting. However, long antisense arms could critically influence a pre-equilibrium of the cleavage reaction, which would reduce the effective cleavage rates (12). We therefore conclude that the minimal kinetic reaction scheme for catalytic antisense RNAs as shown in Figure 1 has to be augmented by an additional step for the required conformational change, as has been proposed based on kinetic data for short hammerhead ribozymes (30). In this context it is also interesting that the cleavage rates (k_{cat}) obtained with conventional hammerhead ribozymes are reduced from ~1/min with short model substrate RNAs to about 0.01–0.001/min when long substrate RNAs are used instead (summarized in 49; reviewed in 31), indicating a similar inhibition of structural rearrangement by increased friction caused by the long substrate RNA. Addition of spermidine might also bring complexes of long substrate RNAs with short hammerhead ribozymes into the 'equiangular' intermediate structure and thus accelerate cleavage. In this context it is interesting to note that oligoamines are ubiquitously present in eukaryotic cells. The spermidine concentration is estimated to be between 1 and 2 mM (50), thus providing favourable conditions for hammerhead ribozymes with long antisense arms. Moreover, it should not be forgotten that the plant cell provides, even at a moderate temperature, the appropriate conditions for cleavage by the naturally occurring hammerhead ribozymes, which must be considered as long substrate RNAs.

ACKNOWLEDGEMENTS

We thank Dr D.M.J.Lilley for communicating unpublished results, Dr Gerhard Steger for helpful discussions and Dr Raymond Lee and Michela Denti for critical reading of the manuscript. This work was supported by the European Union by a training grant to C.H. (BIO4-CT96-5079), by grant BIO2CT930400-DG12SSMA and by the Bundesministerium für Bildung, Forschung und Wissenschaft (grant 01 KV 9517).

REFERENCES

1 Bruening,G. (1989) *Methods Enzymol.*, **180**, 546–558.
2 Symons,R.H. (1992) *Annu. Rev. Biochem.*, **61**, 641–671.
3 Fedor,M.J. and Uhlenbeck,O.C. (1992) *Biochemistry*, **31**, 12042–12054.
4 Tabler,M. and Tsagris,M. (1991) *Gene*, **108**, 175–183.
5 Baidya,N. and Uhlenbeck,O.C. (1997) *Biochemistry*, **36**, 1108–1114.
6 Homann,M., Tzortzakaki,S., Rittner,K., Sczakiel,G. and Tabler,M. (1993) *Nucleic Acids Res.*, **21**, 2809–2814.
7 Crisell,P., Thompson,S. and James,W. (1993) *Nucleic Acids Res.*, **21**, 5251–5255.
8 Tabler,M., Tzortzakaki,S., Homann,M. and Sczakiel,G. (1994) *Nucleic Acids Res.*, **22**, 3958–3965.
9 Hormes,R., Homann,M., Oelze,I., Marschall,P., Tabler,M., Eckstein,F. and Sczakiel,G. (1997) *Nucleic Acids Res.*, **25**, 769–775.
10 Hertel,K.J., Herschlag,D. and Uhlenbeck,O.C. (1994) *Biochemistry*, **33**, 3374–3385.
11 Hertel,K.J. and Uhlenbeck,O.C. (1995) *Biochemistry*, **34**, 1744–1749.
12 Homann,M., Tabler,M., Tzortzakaki,S. and Sczakiel,G. (1994) *Nucleic Acids Res.*, **22**, 3951–3957.
13 Zoumadakis,M., Neubert,W.J. and Tabler,M. (1994) *Nucleic Acids Res.*, **22**, 5271–5278.
14 Sambrook,J., Fritsch,E.F. and Maniatis,T. (1989) *Molecular Cloning: A Laboratory Manual*, 2nd Edn. Cold Spring Harbor Laboratory Press, Cold Spring Harbor, NY.
15 Tsagris,M., Tabler,M., Mühlbach,H.-P. and Sänger,H.L. (1987) *EMBO J.*, **8**, 2173–2183.
16 Uhlenbeck,O.C. (1987) *Nature*, **328**, 596–600.
17 Dahm,S.C. and Uhlenbeck,O.C. (1991) *Biochemistry*, **30**, 9464–9469.
18 Dahm,S.C., Derrick,W.B. and Uhlenbeck,O.C. (1993) *Biochemistry*, **32**, 13040–13045.
19 Tuschl,T., Ng,M.M.P., Pieken,W., Benseler,F. and Eckstein,F. (1993) *Biochemistry*, **32**, 11658–11668.
20 Grasby,J.A., Butler,P.J.G. and Gait,M.J. (1993) *Nucleic Acids Res.*, **21**, 4444–4450.
21 Sawata,S., Komiyama,M., and Taira,K. (1995) *J. Am. Chem. Soc.*, **117**, 2357–2358.
22 Takagi,Y., and Taira,K. (1995) *FEBS Lett.*, **361**, 273–276.
23 Sänger,W. (1983) *Principles of Nucleic Acid Structure*. Springer-Verlag, New York, NY.
24 Kuimelis,R.G. and McLaughlin,L.W. (1996) *Biochemistry*, **35**, 5308–5317.
25 Gast,F.-U. and Hagerman,P.J. (1991) *Biochemistry*, **30**, 4268–4277.
26 Persson,C., Wagner,E.G.H. and Nordström,K. (1990) *EMBO J.*, **9**, 3767–3775.
27 Zoumadakis,M. and Tabler,M. (1995) *Nucleic Acids Res.*, **23**, 1192–1196.
28 Clouet-d'Orval,B. and Uhlenbeck,O.C. (1995) *Biochemistry*, **34**, 11186–11190.
29 Sawata,S., Shimayama,T., Komiyama,M., Kumar,P.K.R., Nishikawa,S. and Taira,K. (1993) *Nucleic Acids Res.*, **21**, 5656–5660.
30 Hendry,P. and McCall,M.J. (1995) *Nucleic Acids Res.*, **23**, 3928–3936.
31 Birikh,K.R., Heaton,P.A. and Eckstein,F. (1997) *Eur. J. Biochem.*, **245**, 1–16.
32 Gast,F.-U., Amiri,K.M.A. and Hagerman,P.J. (1994) *Biochemistry*, **33**, 1788–1796.
33 Amiri,K.M.A. and Hagerman,P.J. (1994) *Biochemistry*, **33**, 13172–13177.
34 Amiri,K.M.A. and Hagerman,P.J. (1996) *J. Mol. Biol.*, **261**, 125–134.
35 Bassi,G.S., Møllegaard,N.-E., Murchie,A.I.H., von Kitzing,E. and Lilley, D.M.J. (1995) *Nature Struct. Biol.*, **2**, 45–55.
36 Bassi,G.S., Murchie,A.I.H. and Lilley,D.M.J. (1996) *RNA*, **2**, 756–768.
37 Menger,M., Tuschl,T., Eckstein,F. and Pörschke,D. (1996) *Biochemistry*, **35**, 14710–14716.
38 Heus,H.A. and Pardi,A. (1991) *J. Mol. Biol.*, **217**, 113–124.
39 Orita,M., Vinayaka,R., Andrus,A., Warashina,M., Chiba,A., Kaniwa,H., Nishikawa,F., Nishikawa,S. and Taira,K. (1996) *J. Biol. Chem.*, **271**, 9447–9454.
40 Long,D.M., LaRiviere,F.J. and Uhlenbeck,O.C. (1995) *Biochemistry*, **34**, 14435–14440.
41 Shimayama,T., Nishikawa,S. and Taira,K. (1995) *FEBS Lett.*, **368**, 304–306.
42 Guerrier-Takada,C., Gardiner,K., Marsh,T., Pace,N. and Altman,S. (1983) *Cell*, **35**, 849–857.
43 Kapahnke,R., Rappold,W., Desselberger,U. and Riesner,D. (1986) *Nucleic Acids Res.*, **14**, 3215–3228.
44 Pley,H.W., Flaherty,K.M. and McKay,D.B. (1994) *Nature*, **372**, 68–74.
45 Tuschl,T., Gohlke,C., Jovin,T.M., Westhof,E. and Eckstein,F. (1994) *Science*, **266**, 785–789.
46 Scott,W.G., Finch,J.T. and Klug A. (1995) *Cell*, **81**, 991–1002.
47 Hagerman,P.J. and Amiri,K.M.A. (1996) *Curr. Opin. Struct. Biol.*, **6**, 317–321.
48 Scott,W.G., Murray,J.B., Arnold,J.R.P., Stoddard,B.L. and Klug,A. (1996) *Science*, **274**, 2065–2069.
49 Sczakiel,G. (1996) In Eckstein,F. and Lilley,D.M.J. (eds), *Nucleic Acids and Molecular Biology*. Springer-Verlag, Berlin, Germany, Vol. 10, pp. 231–242.
50 Russell,D.H. (1983) *Crit. Rev. Clin. Lab. Sci.*, **18**, 261–311.